The Transmission of the Electronic Character of Guanin-9-yl Drives the Sugar–Phosphate Backbone Torsions in Guanosine 3′,5′-Bisphosphate**

Parag Acharya, Anna Trifonova, Christophe Thibaudeau, András Földesi, and Jyoti Chattopadhyaya*

The intrinsic dynamics and architectural flexibility of nucleic acids,[1a] manifesting into specific biological function, are the result of cooperativity of its three essential components: the pentofuranose, the nucleobase, and the phosphodiester. We have earlier shown that the interplay and balance of stereoelectronic *gauche*[2a–e, g, h] and anomeric effects[2g, h, j] energetically drive the two-state pseudorotational equilibrium between north-type (*N*, C2′-*exo*-C3′-*endo*) and south-type (*S*, C3′-*exo*-C2′-*endo*)[1a, 2b, g, 3] (*N* ⇌ *S*, Scheme 1). These works have subsequently led to a detailed dissection[2] of various

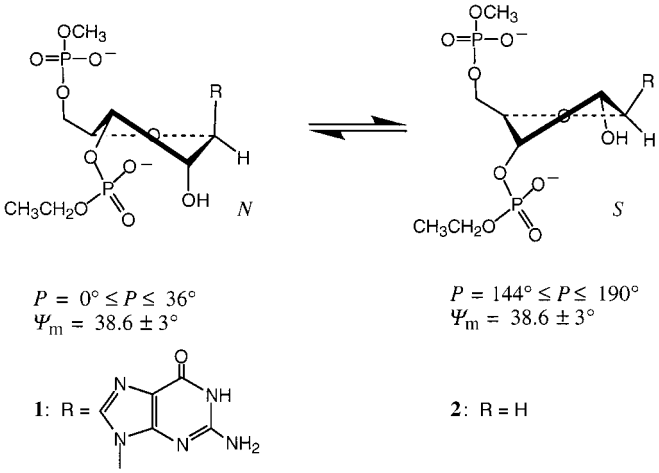

Scheme 1. Schematic representation of the dynamic two-state *N* ⇌ *S* pseudorotational equilibrium[1a, 2b, g, 3] of the β-D-pentofuranose moiety, which is influenced by the nature and relative orientation of the substituents through the *gauch* and anomeric effects.[2, 3a] *P* = phase angle, Ψ_m = puckering amplitude.

gauche and anomeric forces which are dictated by the electronic nature of various pentose sugar substituents. The chemical nature of many of these sugar substituents (especially aglycone and the phosphate) can be altered and tuned by the pH of the medium as well by the complexes formed between the nucleotide and the ligand present in the solution.

We herein report our studies on the pD-dependent conformational analysis of guanosine 3′,5′-bisphosphate (EtpGpMe, **1**) as a model mimicking the central nucleotide moiety in a trinucleoside diphosphate in a single-stranded RNA. A complete interdependency with respect to conformational preference has been found for the sugar *N* ⇌ *S* pseudorotational[1a, 2] and phosphate $\varepsilon^t \rightleftharpoons \varepsilon^-$ equilibria[1a, 2j] in **1**, as the protonation ⇌ deprotonation equilibrium at the N7 basic site[2j] of guanin-9-yl in **1** changes as a function of pH; such an effect is completely absent in the apurinic counterpart [Etp(AP)pMe] (**2**). It has been demonstrated that as the electronic character of the guanine moiety in **1** changes with the protonation ⇌ deprotonation equilibrium,[2j] the strength of the anomeric effect ($n_{O4'} \rightarrow \sigma^*_{C1'-N9}$ orbital mixing[2g, h, j, 3a, 4]) is continuously modulated to induce a change in the electron-density potential of O4′ (tunable $n_{O4'} \rightarrow \sigma^*_{C1'-N9}$ orbital mixing). This, in turn, dictates the nature of the orbital overlap of $\sigma_{C3'-H3'}$ with $\sigma^*_{C4'-O4'}$ as well as the stabilization energy of the newly formed hybrid orbitals (the 3′-*gauche* effect: $\sigma_{C3'-H3'} \rightarrow \sigma^*_{C4'-O4'}$ orbital mixing[2g, 3a, 5]). As the 3′-*gauche* effect becomes effective, the charge density at C3′ changes, which further influences the electron-density potential of O3′ and consequently the ability of its lone pair orbital to overlap with the antibonding orbital of P3′–O(ester) (a tunable anomeric transmission of $n_{O3'} \rightarrow \sigma^*_{P3'-O(ester)}$). This tunable transmission of the charge density from the aglycone, turning the conformational wheel across the sugar–phosphate backbone, is influenced by the relative donor–acceptor capabilities of bonding, nonbonding, and antibonding orbitals of various sugar atoms and substituents. This is conceptually very similar to the through-space transport of charge or electrons by stacked nucleic acid aglycones in conventional nucleic acid molecular wires,[1b, c] except for the fact that the nucleic acid chain is damaged in the latter upon transport of electrons through the stacked nucleobases in a distance-dependent manner. In contrast, in the former the conformational wheel is turned by tunable change of the electron-density potential of various donor and acceptor orbitals by both through-space and through-bond effects.

The basis of our analysis is as follows: The mole fractions of *N*- and *S*-type conformers from pD 1.0–6.7 have been extracted by pseudorotational analysis[2, 3a, 6–8] of temperature-dependent $^3J_{H,H}$ coupling constants with the PSEUROT program (version 5.4)[7] using a generalized Karplus-type equation.[8a, b] The values for ΔG^0 of the two-state *N* ⇌ *S* pseudorotational equilibrium at seven pD levels between 6.7 and 1.0 were obtained (Table 1). As the medium becomes more acidic, N7 of the guanin-9-yl group becomes protonated[2j] and the electron density at N9 is reduced, causing an increase in the strength of the anomeric effect ($n_{O4'} \rightarrow \sigma^*_{C1'-N9}$ orbital mixing).[2g, h, j] The conformational outcome of this is that the aglycone takes up the pseudoaxial orientation and the *N* ⇌ *S* pseudorotational equilibrium for **1** is gradually shifted towards *N*-type (78% *S* at pD 6.7 to 53% *S* at pD 1.6), which is reflected by a change in ΔG^0 (at 298 K) from −3.2 kJ mol^{-1} at pD 6.7 to 0.0 kJ mol^{-1} at pD 1.0 (Table 1).

[*] Prof. J. Chattopadhyaya, P. Acharya, A. Trifonova, C. Thibaudeau, A. Földesi
Department of Bioorganic Chemistry, Box 581, Biomedical Centre
University of Uppsala
S-751 23 Uppsala (Sweden)
Fax: (+46) 185-54-495
E-mail: jyoti@bioorgchem.uu.se

[**] We thank the Swedish Board for Technical Development (TFR), the Swedish Natural Science Research Council (NFR), and the Swedish Board for Technical Development (NUTEK) for generous financial support. Thanks are due to the Wallenbergstiftelsen, Forskningsrådsnämnden and the University of Uppsala for funds to purchase of 500-MHz and 600-MHz Bruker DRX NMR spectrometers.

Supporting information for this article is available on the WWW under http://www.wiley-vch.de/home/angewandte/ or from the author.

Table 1. Determination of ΔG^0 values (at 298 K) of two-state $N \rightleftharpoons S$ and $\varepsilon^t \rightleftharpoons \varepsilon^-$ equilibria at different pD values from pseudorotational analyses and EPSILON calculations, respectively, as well as the percentage population of γ^+ and β^t conformers at 298 K for EtpGpMe (**1**)[a].

	$N \rightleftharpoons S$		$\varepsilon^t \rightleftharpoons \varepsilon^-$		β^t[%]	γ^+[%][c]
pD	ΔG^{298} (σ)[b]	S[%]	ΔG^{298} (σ)[b]	ε^-[%]		
1.0[d]	−0.0 (0.1)	–	0.3 (0.2)	–	–	–
1.6	−0.3 (0.2)	53	0.2 (0.2)	48	78	77
2.0	−0.7 (0.2)	58	0.0 (0.5)	50	79	78
2.4	−1.4 (0.2)	64	−1.2 (0.2)	62	79	74
2.7	−2.3 (0.2)	72	−1.7 (0.2)	66	80	73
3.0	−2.4 (0.2)	72	−1.8 (0.2)	67	80	71
6.7	−3.2 (0.2)	78	−2.0 (0.2)	69	81	72

[a] For the experimental procedure used to calculate the values, see the Supporting Information. [b] Values for ΔG^{298} (in kJ mol^{-1}) of the $N \rightleftharpoons S$ and $\varepsilon^t \rightleftharpoons \varepsilon^-$ equilibria were calculated directly from the average logarithm $\ln_{av}(x_a/(1-x_a))$ by using the Gibbs equation $\Delta G^T = -(RT/1000)\ln_{av}(x_a/(1-x_a))$ with $1-x_a = x_b$, where $x_a = x_S$ or $x_a = x_{\varepsilon^-}$ and $x_b = x_N$ or $x_b = x_{\varepsilon^t}$; R is the gas constant, and T is the temperature. The standard deviations (σ) are given in parentheses. [c] Calculated from the sum of $^3J_{H5',P5'}$ and $^3J_{H5'',P5'}$; the proton signals are assigned as downfield shift of δ(H5′) and upfield shift of δ(H5″). [d] Due to the overlapping of the H3′ peak with the signal for residual water (298 K, pD 1.0), the coupling constants could not be used for conformational analyses. To calculate ΔG^{298} the value of $\ln_{av}(x_a/(1-x_a))$ at pD 1.0 has been extrapolated from the values at $T = 288$ K and $T = 303$ K.

The plot of ΔG^0[2g, i–k] for the $N \rightleftharpoons S$ equilibrium in **1** as a function of pD (Figure 1 A) has the typical sigmoidal shape with an inflection point at 2.4, which is identical to the the pK_a of the constituent guanin-9-yl, determined independently from the plot of δ(H8) as a function of pD (Figure 1 B). Noteworthy is that such sigmoidal plots have been found earlier for β-D-2′,3′-dideoxynucleosides,[2i] 2′-deoxynucleosides,[2i] and ribo *N*- or *C*-nucleosides[2k] as well as some α-D-2′,3′-dideoxynucleosides[2i] and 2′-deoxynucleosides.[2i] The pK_a value for **1** was confirmed by the Hill plot[2g, i–k] (Figure S1 in the Supporting Information), which was characteristic of a single protonation site. In a control experiment, the difference in $^3J_{H,H}$ at neutral and acidic pD values at 298 K (Table S4 in the Supporting Information) was found to be negligible (± 0.1 Hz over the pD range studied) for **2**, showing that in the absence of the aglycone, the $N \rightleftharpoons S$ equilibrium is unbiased and remains unchanged at all pD values.

Since the ε^+ conformer with respect to the C3′–O3′ bond is energetically forbidden,[9a] and is not found in the crystal structure,[9b] the temperature-dependent $^3J_{C4',P3'}$, $^3J_{C2',P3'}$, and $^3J_{H3',P3'}$ experimental coupling constants for **1** have been interpreted in terms of a two-state $\varepsilon^t \rightleftharpoons \varepsilon^-$ equilibrium; this gives the temperature-dependent mole fractions upon use of the program EPSILON[2c, f, 9, 10] (see the Supporting Information). The logarithm of the ratio of the resulting mole fractions of ε^- and ε^t gave ΔG^0 at 298 K for the $\varepsilon^t \rightleftharpoons \varepsilon^-$ equilibrium in **1** at seven pD values between 6.7 and 1.0; ΔG^{298} varied from -2.0 to $+0.3$ kJ mol^{-1} (Table 1) for the population of ε^-, decreasing from 69 % at pH 6.7 for neutral guanine to 48 % at pH 1.6 for N7-protonated guanine. In the case of our reference compound **2** no change in $^3J_{H,P}$ and $^3J_{C,P}$ was observed (Table S4 in the Supporting Information), thereby allowing us to conclude that the conformational changes observed with respect to C3′–O3′ in **1** over the pD range studied is a result of a modulation of the electronic

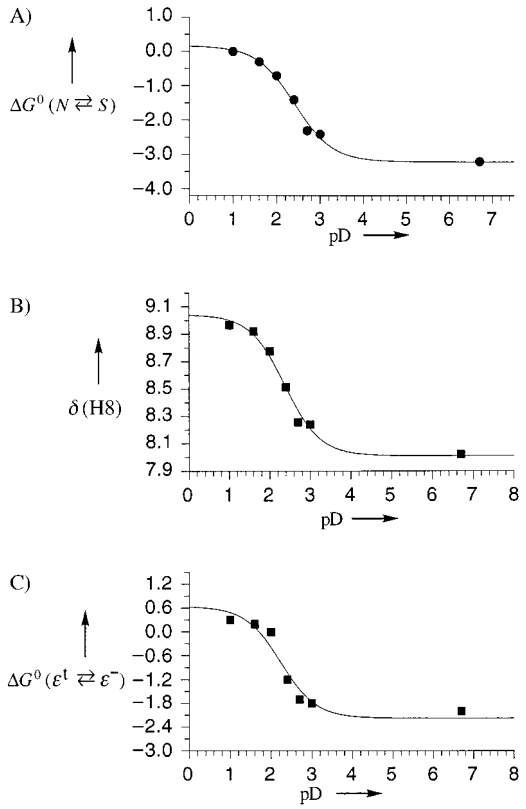

Figure 1. Plots of ΔG^0 [kJ mol^{-1}] for the $N \rightleftharpoons S$ pseudorotational equilibrium of the pentofuranse moiety (A), the chemical shift of H8 of the guanin-9-yl nucleobase (B), and ΔG^0 [kJ mol^{-1}] of the $\varepsilon^t \rightleftharpoons \varepsilon^-$ equilibrium of the 3′-ethylphosphate group in **1** (C) as a function of pD at 298 K. The sigmoidal curves result from the best iterative least-square fit of $\Delta G^0(N \rightleftharpoons S)$, δ(H8), and $\Delta G^0(\varepsilon^t \rightleftharpoons \varepsilon^-)$ values to the Henderson–Hasselbalch equation (see the Supporting Information); pD at the inflection point: A) 2.4, B) 2.4, C) 2.3. See text for further details.

character of the neutral guanine moiety upon protonation to guanine-N7H$^+$. Interestingly, the plot of ΔG^0 as a function of pD for the $\varepsilon^t \rightleftharpoons \varepsilon^-$ equilibrium for **1** also gives a sigmoidal curve (Figure 1 C). The pD value of 2.3 at the inflection point is nearly identical (i.e., within the accuracy of the measurements) to the pK_a value of 2.4 for the guanin-9-yl group in **1**; this was also conformed by the Hill plot analysis[2g, i–k] (Figure S1 in the Supporting Information). Thus, the pD-dependent conformational reorientation of the C3′–O3′ bond (reflected by ΔG^0 values for the $\varepsilon^t \rightleftharpoons \varepsilon^-$ equilibrium) is directly dictated by the pK_a of the constituent C1′-aglycone in **1**.

The correlation plot of ΔG^0 for the N $\rightleftharpoons$ S equilibrium of the pentofuranose sugar as a function of ΔG^0 for the $\varepsilon^t \rightleftharpoons \varepsilon^-$ equilibrium of the 3′-phosphate moiety in **1** gives a straight line with a high Pearson correlation coefficient ($R = 0.97$, Figure 2 A). This means that as the guanin-9-yl nucleobase in **1** is gradually protonated in the acidic medium, and the modulation of the strength of the anomeric effect shifts the $N \rightleftharpoons S$ equilibrium toward *N*, which in turn dynamically shifts the $\varepsilon^t \rightleftharpoons \varepsilon^-$ equilibrium towards ε^t relative to the situation at neutral pD. Additional evidence that the transmission of the free energy of the protonation $\rightleftharpoons$ deprotonation equilibrium steers the phosphate conformation by changing the conformation of the sugar moiety is that the plots of $\Delta G^0(N \rightleftharpoons S)$

  1433-7851/99/3824-3646 $ 17.50+.50/0 *Angew. Chem. Int. Ed.* **1999**, *38*, No. 24

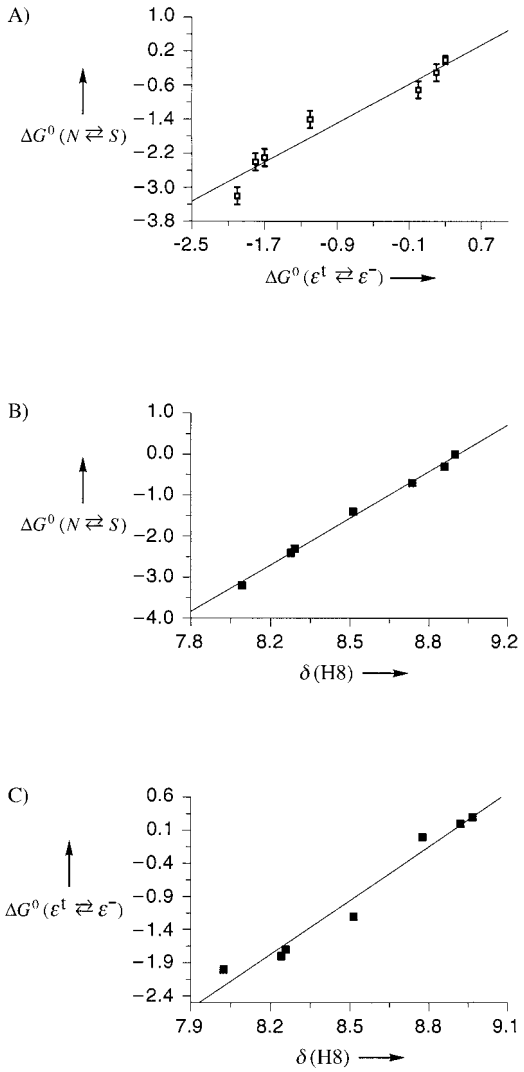

Figure 2. A) The plot of ΔG^0 [kJ mol^{-1}] for the $N \rightleftharpoons S$ pseudorotational equilibrium at 298 K for **1** as a function of ΔG^0 [kJ mol^{-1}] for the $\varepsilon^t \rightleftharpoons \varepsilon^-$ equilibrium; $R = 0.97$, slope 1.15 ($\sigma = 0.08$), intercept -0.45 ($\sigma = 0.10$). The vertical bars show the standard deviations at each pD value. B) The plot of ΔG^0 [kJ mol^{-1}] for the $N \rightleftharpoons S$ pseudorotational equilibrium for **1** as a function of δ(H8) at 298 K; $R = 1.00$, slope 3.25 ($\sigma = 0.06$), intercept -29.16 ($\sigma = 0.50$). C) The plot of ΔG^0 [kJ mol^{-1}] for the $\varepsilon^t \rightleftharpoons \varepsilon^-$ equilibrium for **1** as a function of δ(H8) at 298 K; $R = 0.98$, slope 2.70 ($\sigma = 0.14$), intercept -23.96 ($\sigma = 1.16$). In each case the data points are given for the seven pD values investigated.

(Figure 2B) or of $\Delta G^0(\varepsilon^t \rightleftharpoons \varepsilon^-)$ (Figure 2C) in **1** as a function of δ(H8) give straight lines with high correlation coefficients ($R \geq 0.97$).

Consistent with our earlier observation on ribonucleoside 3′-ethylphosphates[2f] at neutral pH and room temperature, we found that the methylene protons of the 3′-ethyphosphate moiety in **1** are nonequivalent owing to the 2′-OH-promoted hydrogen bonding with the vicinal O3′ atom. Hence all our ΔG^0 measurements were performed well below the hydrogen-bond melting temperature for **1** (298 K). This means that all changes of free-energy observed at 298 K for **1** (Table 1) as the pH value is changed are attributed to the free-energy changes of the protonation $\rightleftharpoons$ deprotonation equilibrium of the aglycone to drive the sugar–phosphate backbone in a concerted manner.

As the pD-tunable change of the electronic character of the nucleobase tunes the strength of the anomeric effect, an increased preference for the *N*-type sugar conformation is imposed because of enhanced $n_{O4'} \rightarrow \sigma^*_{C1'-N9}$ orbital interaction.[2g, h, j, 3a, 4] This in turn affects the strength of the O3′-C3′-C4′-O4′ *gauche* effect by retuning the energy levels of the donor and acceptor orbitals in the $\sigma_{C3'-H3'} \rightarrow \sigma^*_{C4'-O4'}$ interaction.[2g, 3a, 5] The extent of $\sigma_{C3'-H3'} \rightarrow \sigma^*_{C4'-O4'}$ participation influences the electron density at O3′, which in turn modulates the O3′-P3′-O anomeric effect[3a, 11] (a tunable transmission of the $n_{O3'} \rightarrow \sigma^*_{P3'-O(ester)}$ orbital interaction, Figure 3, next page).[12] It is noteworthy that the stereoelectronic transmission takes place from the aglycone to the sugar to the phosphate, and not in the reverse direction. The proof of this one-way transmission of stereoelectronic information in **1** is two-fold: 1) The pK_a value of the guanin-9-yl aglycone remains around 2.4, and is independent of any OH or phosphate substituents in the sugar moiety. Thus the pK_a values of N7 are as follows for a series of guanine nucleosides (within the error limits of our NMR experiments):[2] 2′,3′-dideoxyguanosine (pK_a 2.5), 2′-deoxyguanosine (pK_a 2.3), guanosine (pK_a 2.1), and **1** (pK_a 2.4). 2) When the 3′-phosphate (p$K_a \approx 1.5$) in **2** is partially protonated at pD 1.6 under our experimental condition, the coupling constant $^3J_{H,H}$ for the endocyclic sugar moiety remains unaltered, which is in contrast to the situation for **1**. This suggests that the change in the electronic character of the phosphate does not influence the structural and dynamic character of the sugar moiety.

The conformational equilibrium across the γ^+ torsion[13a] (at 298 K) changes from 72% at pD 6.7 to 77% at pD 1.6, which is correlated with δ(H8) for **1** (Figure 4A) as a manifestation of the O4′-C4′-C5′-O5′ *gauche* effect. There is, however, no propagation of this transmission further along the β(C4′-C5′-O5′-P5′) torsion. Similarly the ratio of *syn* and *anti* conformers[13b] does not change as a function of pH, suggesting that

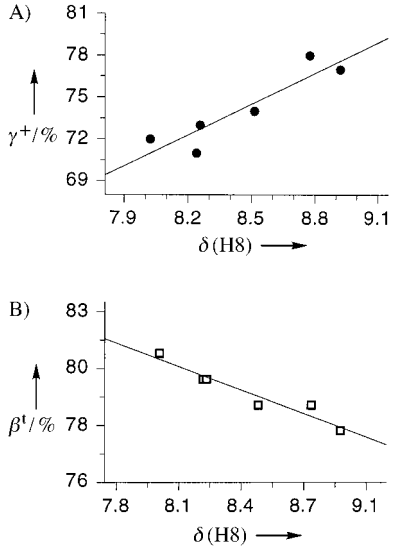

Figure 4. A) The plot of percentage population of γ^+ conformer in **1** (taking H5′ downfield and H5″ upfield) as a function of δ(H8) at different pD values; $R = 0.91$, slope 7.37 ($\sigma = 0.99$), intercept 11.88 ($\sigma = 8.37$). B) The plot of percentage population of β^t conformer in **1** as a function of δ(H8) at different pD values; $R = 0.96$, slope -2.93 ($\sigma = 0.25$), intercept 104.25 ($\sigma = 2.07$).

  1433-7851/99/3824-3647 $ 17.50+.50/0

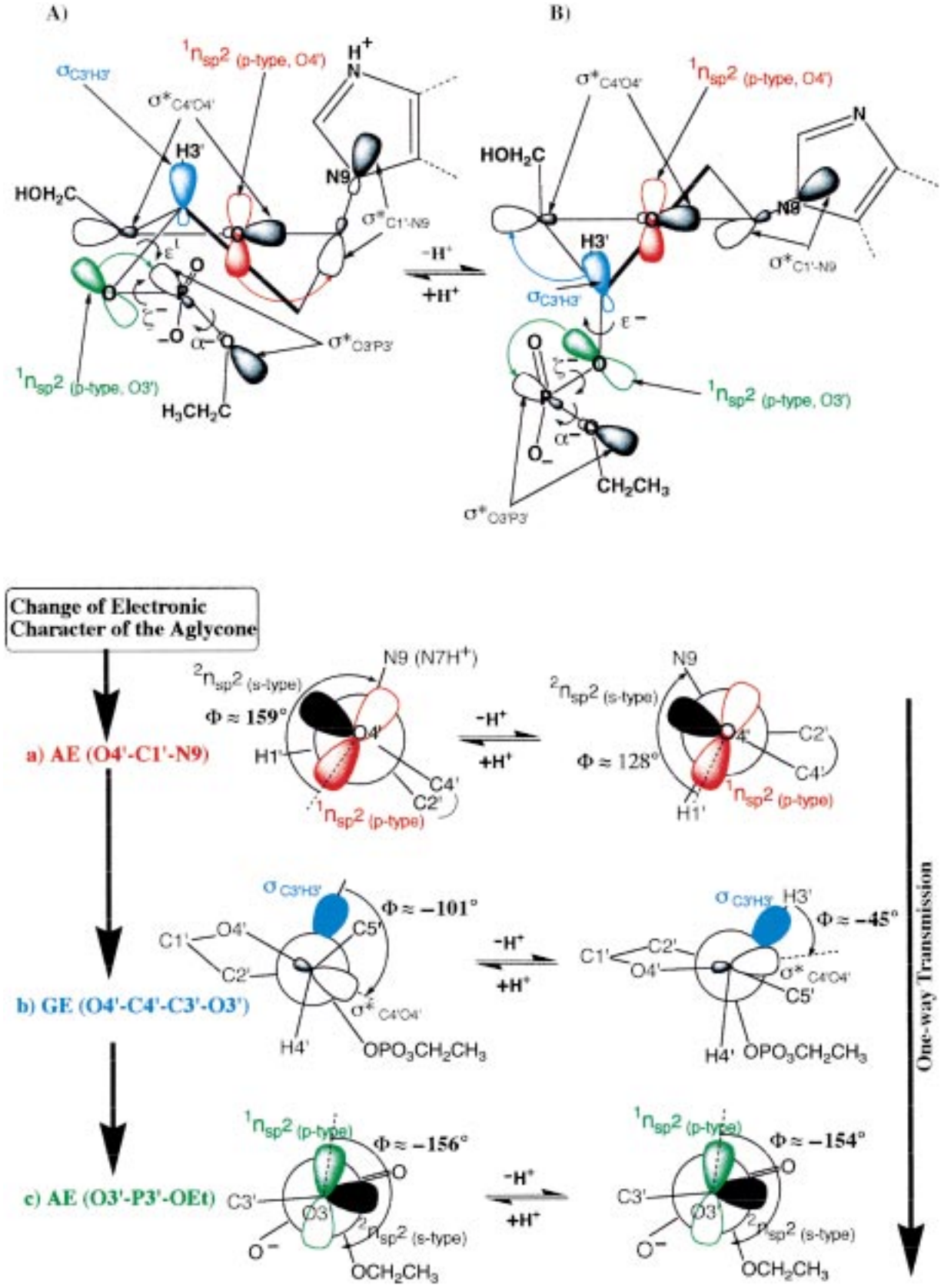

Figure 3. The demonstration of RNA molecular wires using the model EtpGpMe (**1**). Transmission of the free energy of the protonation $\rightleftharpoons$ deprotonation equilibrium of the guanin-9-yl group in **1** drives the sugar–phosphate conformations through three consecutive stereoelectronic tunings (a–c; AE = anomeric effect, GE = *gauche* effect). Appropriate orbital overlap and the energy difference between the donor and acceptor orbitals, dictated by various sugar atoms and substituents, drive the sugar–phosphate conformation through the interplay of *gauche* and anomeric effects. All orbitals are shown by straight arrows. Smaller curved arrows show the preferred torsional orintation, whereas the larger curved arrows indicate the mixing of donor and acceptor orbitals. See reference [12] for further details.

  1433-7851/99/3824-3648 $ 17.50+.50/0

protonation of the aglycone has no measurable effect on the orientation of the glycosyl torsion. On the other hand, plots of the pH-dependent ^{31}P chemical shift of the 3′-phosphate moiety in **1** as function of ΔG^0 for the $N \rightleftharpoons S$ or $\varepsilon^t \rightleftharpoons \varepsilon^-$ equilibria give straight lines ($R \geq 0.94$, Figure 5A, B), which

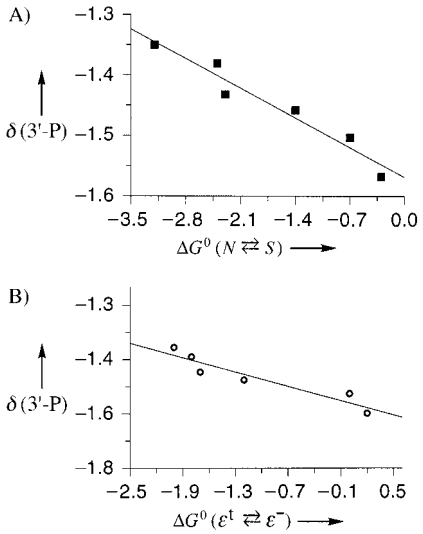

Figure 5. Plots of the ^{31}P chemical shift of the 3′-phospate moiety (δ(3′-P)) in **1** as function of ΔG^0 [kJ mol^{-1}] of the $N \rightleftharpoons S$ pseudorotational equilibrium (A; $R = 0.97$, slope -0.07 ($\sigma = 0.01$), intercept -1.62 ($\sigma = 0.01$)) and of ΔG^0 [kJ mol^{-1}] of the $\varepsilon^t \rightleftharpoons \varepsilon^-$ equilibrium (B; $R = 0.94$, slope -0.08 ($\sigma = 0.01$), intercept -1.58 ($\sigma = 0.01$)) at different pD values.

is not the case with the 5′-phosphate group (see the Supporting Information). This shows that the stereoelectronic transmission is more effective at the 3′ end than at the 5′ end.

Received: June 10, 1999 [Z13543IE]
German version: *Angew. Chem.* **1999**, *111*, 3861 – 3866

Keywords: conformation analysis · NMR spectroscopy · nucleotides · protonations · RNA

[1] a) W. Saenger, *Principles of Nucleic Acid Structure*, Springer, Berlin, **1988**; b) R. E. Peter, J. Dandliker, J. K. Barton, *Angew. Chem.* **1997**, *109*, 2830 – 2848; *Angew. Chem. Int. Ed. Engl.* **1997**, *36*, 2714 – 2730; c) E. Meggers, D. Kusch, M. Spichty, U. Wille, B. Giese, *Angew. Chem.* **1998**, *110*, 507 – 510; *Angew. Chem Int. Ed.* **1998**, *37*, 460 – 465.

[2] a) L. H. Koole, H. M. Buck, A. Nyilas, J. Chattopadhyaya, *Can. J. Chem.* **1987**, *65*, 2089; b) J. Plavec, W. Tong, J. Chattopadhyaya, *J. Am. Chem. Soc.* **1993**, *115*, 9734; c) J. Plavec, C. Thibaudeau, G. Viswanadham, C. Sund, J. Chattopadhyaya, *J. Chem. Soc. Chem. Commun.* **1994**, 781; d) C. Thibaudeau, J. Plavec, N. Garg, A. Papchikhin, J. Chattopadhyaya, *J. Am. Chem. Soc.* **1994**, *116*, 4038; e) J. Plavec, C. Thibaudeau, J. Chattopadhyaya, *J. Am. Chem. Soc.* **1994**, *116,* 6558; f) J. Plavec, C. Thibaudeau, G. Viswanadham, C. Sund, A. Sandstrom, J. Chattopadhyaya, *Tetrahedron* **1995**, *51*, 11775, and references therein; g) C. Thibaudeau, J. Plavec, J. Chattopadhyaya, *J. Org. Chem.* **1996**, *61*, 266; h) J. Plavec, C. Thibaudeau, J. Chattopadhyaya, *Pure Appl. Chem.* **1996**, *68*, 2137; i) C. Thibaudeau, A. Földesi, J. Chattopadhyaya, *Tetrahedron* **1997**, *53*, 14043; j) I. Luyten, C. Thibaudeau, J. Chattopadhyaya, *J. Org. Chem.* **1997**, *62*, 8800; k) I. Luyten, C. Thibaudeau, J. Chattopadhyaya, *Tetrahedron* **1997**, *53*, 6433; l) C. Thibaudeau, J. Plavec, J. Chattopadhyaya, *J. Org. Chem.* **1998**, *63*, 4967.

[3] a) Review: C. Thibaudeau, J. Chattopadhyaya, *Stereoelectronic Effects in Nucleosides and Nucleotides and Their Structural Implications*, Uppsala University Press, **1999**, pp. 27 – 29 (for the two-state $N \rightleftharpoons S$ pseudorotational equilibrium model), 5 – 23 (for anomeric and *gauche* effects); b) H. P. M. de Leeuw, C. A. G. Haasnoot, C. Altona, *Isr. J. Chem.* **1980**, *20*, 108.

[4] a) P. A. Petillo, L. A. Lerner in *The Anomeric Effect and Associated Stereoelectronic Effects* (Ed.: G. R. J. Thatcher), ACS, Washington DC, **1993**, p. 156, and references therein; b) C. L. Perrin, K. B. Armstrong, M. A. Fabian, *J. Am. Chem. Soc.* **1994**, *116*, 715.

[5] a) P. Dionne, M. St.-Jacques, *J. Am. Chem. Soc.* **1987**, *109*, 2616; b) K. B. Wiberg, *Acc. Chem. Res.* **1996**, *29*, 229, and references therein.

[6] a) C. Altona, M. Sundaralingam, *J. Am. Chem. Soc.* **1972**, *94*, 8205; b) C. Altona, M. Sundaralingam, *J. Am. Chem. Soc.* **1973**, *95,* 2333.

[7] a) F. A. A. M. De Leeuw, C. Altona, *J. Comput. Chem.* **1983**, *4*, 428; PSEUROT, QCPE program no. 463, Department of Chemistry, University of Leiden, The Netherlands, **1989**; b) C. A. G. Haasnoot, F. A. A. M. de Leeuw, C. Altona, *Tetrahedron* **1980**, *36*, 2783.

[8] a) E. Diez, J. S. Fabian, J. Guilleme, C. Altona, L. A. Donders, *Mol. Phys.* **1989**, *68*, 49; b) L. A. Donders, F. A. A. M. de Leeuw, C. Altona, *Magn. Reson. Chem.* **1989**, *27*, 556; c) C. Altona, J. H. Ippel, A. J. A. W. Hoekzema, C. Erkelens, G. Groesbeek, L. A. Donders, *Magn. Reson. Chem.* **1989**, *27*, 564; d) J. van Wijk, unpublished results.

[9] a) M. M.Dhingra, A. Saran, *Biopolymers* **1982**, *21*, 859; b) P. P. Lankhorst, C. A. G. Haasnoot, C. Erkelens, C. Altona, *J. Biomol. Struct. Dyn.* **1984**, *1*, 13870; c) M. J. J. Blommers, D. Nanz, O. Zerbe, *J. Biomol. NMR* **1994**, *4*, 595.

[10] a) W. H. Press, B. P. Flannery, S. A. Tenkolsky, W. T. Vatterling, *Numerical recipes (Fortran version)*, Cambridge University Press, New York, **1999**; b) M. M. W. Mooren, S. S. Wijmenga, G. A. van der Marel, J. H. van Boom, C. W. Hilbers, *Nucleic Acids Res.* **1994**, *22*, 2658; c) J. Plavec, J. Chattopadhyaya, *Tetrahedron* **1995**, *36*, 1949.

[11] See reference [1a], pp. 93 – 96, and references therein for the anomeric effect across the 3′O-P-O-ester fragment in the sugar – phosphate backbone.

[12] The energy stabilization through either *gauche* or anomeric effects, manifested by the interaction between the participating donor and the acceptor orbitals, is directly proprtional to the square of the overlap between the donor and the acceptor orbitals (i.e., S^2) as well as inversely proportional to their energy differences (stabilization by AE or $GE = S^2/\Delta E$).[2g, h, j, 3a, 4] When the aglycone is protonated at N7 (Figure 3A), the *N*-type pseudorotamers are preferred owing to the strengthening of the O4′-C1′-N9 anomeric effect, as shown by the overlap between the $^1n_{sp^2}$ orbital of one of the O4′ lone pairs and the antibonding orbital of the C1′–N9 bond ($\sigma^*_{C1'-N9}$). This is illustarted through a Newman projection (Figure 3a), where O4′ lone pair orbitals (higher energy $^1n_{sp^2(p\text{-}type)}$, lower energy $^2n_{sp^2(s\text{-}type)}$) and the $n_{O4'} \rightarrow \sigma^*_{C1'-N9}$ overlap stabilizes the *N*-type over the *S*-type sugars. For an *N*-type sugar, $n_{O4'} \rightarrow \sigma^*_{C1'-N9}$ interactions are possible owing to a near antiperiplanar orientation of $^1n_{sp^2(p\text{-}type)}$ with respect to the C1′–N9 bond ($\Phi(^1n_{sp^2(p\text{-}type)}\text{-}O4'\text{-}C1'\text{-}N9) \approx 159^\circ$), which takes place when the aglycone is pseudoaxial. In contrast, they are much weaker when the aglycone is pseudoequatorial in the *S*-type sugars owing to relatively large deviation from antiplanarity, as indicated by smaller Φ values ($\Phi(^1n_{sp^2(p\text{-}type)}\text{-}O4'\text{-}C1'\text{-}N9) \approx 128^\circ$). On the other hand, in the neutral state (Figure 3B) the *S*-type pseudorotamers are relatively preferred owing to the absence of an O4′-C1′-N9 anomeric effect as well as due to the stabilization through the O3′-C3′-C4′-O4′ *gauche* effect (i.e., the overlap of $\sigma_{C3'-H3'}$ with $\sigma^*_{C4'-O4'}$). In the Newman projection (Figure 3b), the most efficient overlap of the best donor ($\sigma_{C3'-H3'}$) and best acceptor orbitals ($\sigma^*_{C4'-O4'}$) is indicated by a preference for the *gauche* orientation (smaller value for $\Phi(\sigma_{C3'-H3'}\text{-}C3'\text{-}C4'\text{-}\sigma^*_{C4'-O4'}) = -45^\circ$) in the *S*-type sugar over the *trans* conformer (higher value of $\Phi(\sigma_{C3'-H3'}\text{-}C3'\text{-}C4'\text{-}\sigma^*_{C4'-O4'}) = -110^\circ$) in the *N*-type sugar. Thus, in the *S*-type conformation, a reduction of charge density at the O3′ lone pair ($^1n_{sp^2(p\text{-}type)}$) takes place owing to its maximal interaction with $\sigma^*_{C4'-O4'}$ (presumably a combination of through-bond and through-space effects are involved in this process), thereby weakening the O3′-P3′-OCH_2CH_3 anomeric effect in the S/ε^- state. Owing to the $n_{O4'} \rightarrow \sigma^*_{C1'-N9}$ overlap (Figure 3A), the O4′ lone pair is relatively more delocalized in the *N*-type conformation, which places the O3′-C3′-C4′-O4′ fragment in the *trans* orientation, preventing the *gauche* effect from being fully operational (the reverse is true when the anomeric effect is weakened in the *S*-type conformation, Figure 3B). Since the 3′-GE is

not fully operational in the *N*-type sugar conformation, the charge density at the O3′ lone pair ($^1n_{sp^2(p\text{-}type)}$, O3′) is fully available to act as a donor and interact through the anomeric effect with the antibonding $\sigma^*_{P3'-O(ester)}$ orbital (AE(O3′-P3′-OCH_2CH_3)[3a, 11]), when C3′–O3′ is in ε^t, O3′–P3′ in ζ^-, and P3′-O5′ in α^- conformations. The Newman projection (Figure 3c) shows that the overlap between the O3′ lone pair orbitals and the $\sigma^*_{P3'-O(ester)}$ orbital ($n_{O3'} \rightarrow \sigma^*_{P3'-O(ester)}$ orbital mixing) stabilizes ε^t over ε^-. This is not only due to an antiperiplanar orientation of $^1n_{sp^2(p\text{-}type)}$ with respect to the P3′–O(ester) bond, as $\Phi(^1n_{sp^2(p\text{-}type)}$-O3′-P3′-$OCH_2CH_3)$ is nearly the same for the two cases, but largely owing to the greater electron density availible at $n_{O3'}$, arising from the absence of 3′-GE in the *N*-type sugar. The conformational parameters used to build up the model structure of *N*, ε^t, ζ^-, α^-, and *S*, ε^-, ζ^-, α^- conformations of **1** to draw the Newman projections are provided in Table S6 in the Supporting Information.

[13] a) C. A. G. Haasnoot, F. A. A. M. de Leeuw, H. P. M. de Leeuw, C. Altona, *Recl. Trav. Chim. Pays-Bas* **1979**, *98*, 576; b) H. Rosemeyer, G. Tóth, B. Golankiewicz, Z. Kazimierczuk, W. Bourgeois, U. Kretschmer, H. P Muth, F. Seela, *J. Org. Chem.* **1990**, *55*, 5784.

"Figure Eight" Cyclooctapyrroles: Enantiomeric Separation and Determination of the Absolute Configuration of a Binuclear Metal Complex**

Andreas Werner*, Martin Michels, Lars Zander, Johann Lex, and Emanuel Vogel*

Dedicated to Professor Karl Schlögl on the occasion of his 75th birthday

Cyclooctapyrroles (octaphyrins), of which compounds **1**–**4** (in each case as the hexadecaethyl derivative, Scheme 1) are representatives, have developed as an unexpected sideline of our research into porphyrin and corrole isomers.[1] It was during studies on the synthesis of the still hypothetical *trans*-corrphycene that a versatile route to such polypyrrole macrocycles and potential ligands unfolded. We found that cyclooctapyrroles are formed as—in many cases dominating—competing products to cyclotetrapyrroles (porphyrin isomers, corroles, porphyrins-(1.0.1.0), and others) when two suitably functionalized dipyrrole components, of which at least one must be a bipyrrole derivative, are subject to an acid-catalyzed MacDonald condensation.[2]

Although **1**, **3**, and **4** (**2** is derived from **1** by dehydrogenation) were originally formed in only minor quantities, these

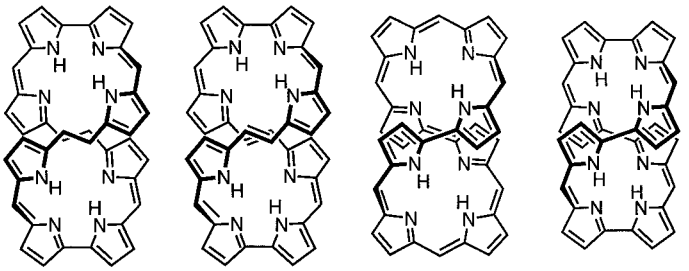

1 **2** **3** **4**

5: Pd–Pd complex **6**: Pd–Pd complex **7**: Cu–Cu complex

several homo- and heterobinuclear complexes have already been prepared[3]

Scheme 1. The figure eight ligands **1**–**4**.

macrocycles are now obtainable in yields of 40, 42, and 25%, respectively (i.e., on a preparative scale), when acid catalysis is replaced by BF_3 catalysis[4] (cyclotetrapyrrole formation is completely suppressed with **1**, **3**, and **4**).

A geometric feature of all previously known cyclooctapyrroles is that—in analogy to Sessler's cyclodecapyrrole turcasarin[5]—both in solution and (where structural analysis is available) in the crystal they exist in a chiral, figure eight conformation of two equidirectional helices (*P*,*P* or *M*,*M*),[6] which, assuming sufficiently restricted mobility, is expected to allow enantiomeric separation. Both **2** and its (according to molecular models) less rigid tetrahydro derivative **1** as well as **3** are highly promising candidates for enantiomeric separation: Based on the observation that the diastereotopicity of the ethyl CH_2 protons remains intact, also in ^{1}H NMR spectra measured at elevated temperature, the inversion barrier of the figure eight loop is expected to be at least 85 kJ mol^{-1}.[1a] In contrast, the NMR study and theoretical calculations[7] show **4** to be a dynamic molecule, even at room temperature, so there is not much chance that stable enantiomers can be obtained.

The cyclooctapyrroles **1**–**4** appear predestined to form binuclear metal complexes since the loop-shaped conformation of these macrocycles exhibits two structurally identical, helical N_4 cavities. Enantiomers of such complexes, which are presumably generally very stable towards racemization owing to the rigidity of the molecule imposed by the incorporation of the metal, are of interest as possible models for binuclear metalloenzymes[8] and as potential catalysts in asymmetric synthesis.[9] In this study, therefore, compounds **1** and **2** as well as their recently obtained palladium and copper complexes **5**–**7** were investigated as examples to effect enantiomeric separation. The success of these efforts is reported here. However, before the separations as such are described in detail, the hitherto still outstanding X-ray structural analyses[10] of **1** and **2** are included and the aforementioned metal complexes of these ligands are described.

According to the analysis, the molecular frameworks of the cyclooctapyrroles **1** and **2** show the figure eight conformation previously derived from the NMR studies (Figure 1a and 1b). As can be seen from the side view of **2** (Figure 1c), the four dipyrrin units are in each case almost planar, so that the helical conformation of the two tetrapyrrole substructures is

[*] Prof. Dr. A. Werner[†]
Institut für Organische Chemie der Universität
Währinger Strasse 38, A-1090 Wien (Austria)
Prof. Dr. E. Vogel, Dr. M. Michels, Dr. L. Zander, Dr. J. Lex
Institut für Organische Chemie der Universität
Greinstrasse 4, D-50939 Köln (Germany)
Fax: (+49) 221-470-5057
E-mail: emanuel.vogel@uni-koeln.de
[†] Died August 23, 1999.

[**] This work was supported by the Deutsche Forschungsgemeinschaft and the Fonds der Chemischen Industrie.

  1433-7851/99/3824-3650 $ 17.50+.50/0